

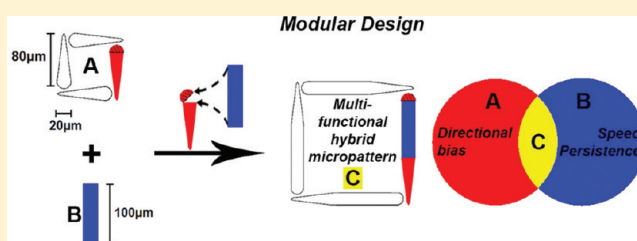
# Modular Design of Micropattern Geometry Achieves Combinatorial Enhancements in Cell Motility

Keiichiro Kushiro and Anand R. Asthagiri\*

Department of Chemical Engineering, Northeastern University, 360 Huntington Avenue, Boston, Massachusetts 02115-5000, United States

## Supporting Information

**ABSTRACT:** Basic micropattern shapes, such as stripes and teardrops, affect individual facets of cell motility, such as migration speed and directional bias, respectively. Here, we test the idea that these individual effects on cell motility can be brought together to achieve multidimensional improvements in cell behavior through the modular reconstruction of the simpler “building block” micropatterns. While a modular design strategy is conceptually appealing, current evidence suggests that combining environmental cues, especially molecular cues, such as growth factors and matrix proteins, elicits a highly nonlinear, synergistic cell response. Here, we show that, unlike molecular cues, combining stripe and teardrop geometric cues into a hybrid, spear-shaped micropattern yields combinatorial benefits in cell speed, persistence, and directional bias. Furthermore, cell migration speed and persistence are enhanced in a predictable, additive manner on the modular spear-shaped design. Meanwhile, the spear micropattern also improved the directional bias of cell movement compared to the standard teardrop geometry, revealing that combining geometric features can also lead to unexpected synergistic effects in certain aspects of cell motility. Our findings demonstrate that the modular design of hybrid micropatterns from simpler building block shapes achieves combinatorial improvements in cell motility. These findings have implications for engineering biomaterials that effectively mix and match micropatterns to modulate and direct cell motility in applications, such as tissue engineering and lab-on-a-chip devices.



Here, we show that, unlike molecular cues, combining stripe and teardrop geometric cues into a hybrid, spear-shaped micropattern yields combinatorial benefits in cell speed, persistence, and directional bias. Furthermore, cell migration speed and persistence are enhanced in a predictable, additive manner on the modular spear-shaped design. Meanwhile, the spear micropattern also improved the directional bias of cell movement compared to the standard teardrop geometry, revealing that combining geometric features can also lead to unexpected synergistic effects in certain aspects of cell motility. Our findings demonstrate that the modular design of hybrid micropatterns from simpler building block shapes achieves combinatorial improvements in cell motility. These findings have implications for engineering biomaterials that effectively mix and match micropatterns to modulate and direct cell motility in applications, such as tissue engineering and lab-on-a-chip devices.

## INTRODUCTION

Micrometer-scale features of the cellular microenvironment profoundly affect cell motility and can be incorporated in biomaterials to modulate cell migration.<sup>1–3</sup> Micropatterned grooves and steps have been used to orient and guide cell movement<sup>4–6</sup> and aid blood-vessel-like tissue formation.<sup>7</sup> Meanwhile, surfaces presenting micropatterned stripes of adhesion proteins have been used to guide axonal growth in neurons and study autoreverse nuclear migration.<sup>8,9</sup> Furthermore, Chien and colleagues observed that endothelial cells confined to narrow stripe patterns acquire a polarized morphology and an enhanced migration speed along the stripes.<sup>10</sup> More recently, Yamada and colleagues found that fibroblasts can also acquire a uniaxial morphology and exhibit enhancements in migration speed when seeded on thin micropatterned stripes that mimic the one-dimensional topography of oriented matrix fibrils.<sup>11</sup>

The effects of individual micropattern designs, however, are restricted typically to certain facets of cell motility. For example, micropatterned stripes enhance cell migration speed and confine movement along a single dimension. However, it is unclear to what extent this confinement affects the time that cells move along a single direction before turning (i.e., persistence time). Moreover, stripe patterns do not control the direction in which cells move along a single axis. On the other hand, we and others have recently shown that asymmetric

micropatterns, such as teardrops, provide a platform to program a direction bias to cell movement.<sup>12–16</sup>

As we begin to better understand the effect of individual micropatterns on particular aspects of cell migration, an emerging challenge is to probe whether micropattern shapes can be mixed and matched to achieve combinatorial, multifaceted enhancements in cell motility. Here, we examine this question by testing whether a hybrid pattern that combines stripe and teardrop geometries can enable both rapid and directed movement. In addition, it is intriguing to hypothesize that cell behavior on the hybrid micropattern shape may be quantitatively predictable from an understanding of cell performance on the original “building block” micropatterns. While a modular approach to micropattern design is appealing conceptually, it is not evident that hybrid geometric cues would yield predictable effects on cell behavior. In fact, other environmental cues that regulate motility, such as growth factors and adhesion peptides, exhibit highly synergistic non-additive effects on cell motility, owing to strong coupling through intracellular signaling networks.<sup>17,18</sup> Whether micrometer-scale geometric cues can be used in a more predictable modular fashion remains to be determined. To begin to

**Received:** December 12, 2011

**Revised:** February 1, 2012

**Published:** February 7, 2012

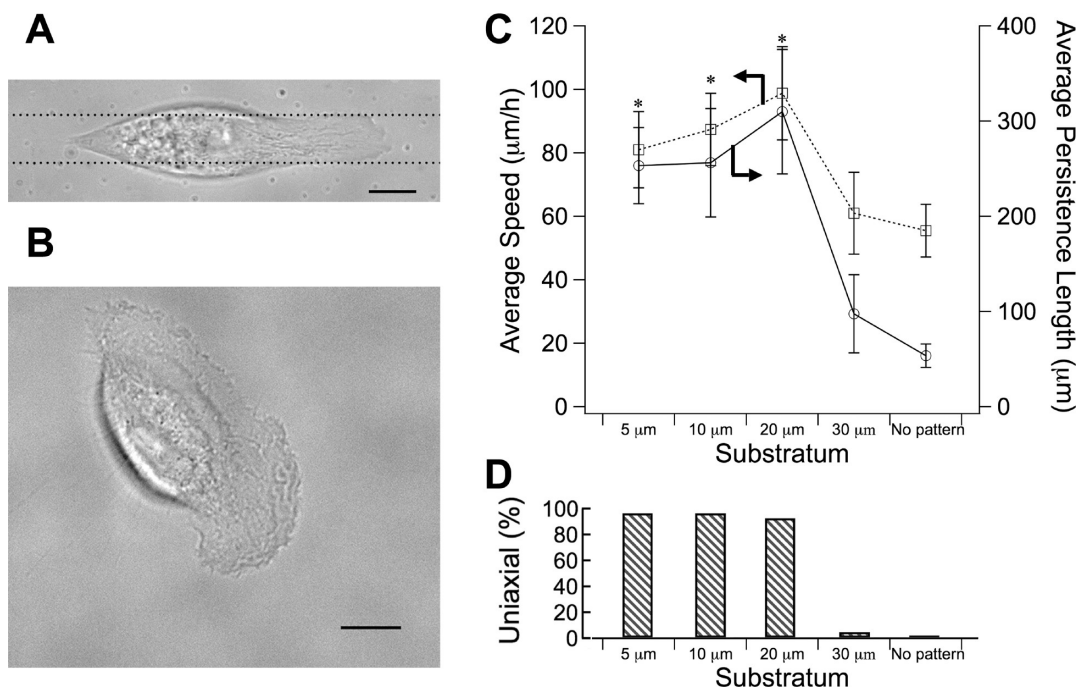


**Figure 1.** Stripe patterns promote uniaxial morphology and enhance the motility of MCF-10A epithelial cells. (A) Representative cell with uniaxial morphology and single lamella; the dotted lines delineate the underlying  $10\ \mu\text{m}$  pattern. (B) Representative cell with broadly shaped lamella and the absence of uniaxial morphology on a nonpatterned substratum. (C) Quantitative analysis of cell motility on stripe patterns. Cell migration speed (left y axis, dotted line) and persistence length (right y axis, solid line) are significantly enhanced on stripe patterns ranging from 5 to  $20\ \mu\text{m}$  stripe widths (\*;  $p < 0.01$  for both persistence and speed when compared to control nonpatterned substratum). (D) Percentages of cells that acquire uniaxial morphology with a single prominent lamella during a 12 h period on stripe patterns of indicated widths or on a nonpatterned substratum. Uniaxial morphology was prevalent on stripe patterns of widths  $20\ \mu\text{m}$  and below. Error bars = standard error of the mean (SEM;  $N = 2\text{--}4$  trials with 10–20 cells quantified per trial). Scale bar =  $10\ \mu\text{m}$ .

examine the modular application of micropattern geometry, we focused in this work on elucidating the effect of combining two building block shapes, teardrops and stripes, on cell motility.

## EXPERIMENTAL SECTION

**Fabrication of Micropatterned Substrates.** Microcontact printing with a polydimethylsiloxane (PDMS) stamp was used to pattern the adhesion ligand, as described previously.<sup>14</sup> Briefly, ultraviolet (UV) light was passed through a chrome mask containing the teardrop- and spear-shaped patterns [Nanoelectronics Research Facility, University of California, Los Angeles (UCLA)] onto a layer of SU-8 negative photoresist (MicroChem) to make a mold, onto which PDMS (Momentive Performance Materials) was cast to make the stamp. 16-Mercaptohexadecanoic acid (Sigma Aldrich) was printed with the stamp onto the gold-coated, chambered coverslide (Fisher Thermo Scientific, NUNC). The unprinted area was passivated using PEG(6)-thiol (Prochimia) to prevent protein adsorption and cell adhesion. The carboxyl group of the acid was catalytically activated using 1-ethyl-3-(3-dimethylaminopropyl)carbodiimide HCl (EDC; Fisher Thermo Scientific, Pierce) and *N*-hydroxysulfosuccinimide (sulfo-NHS; Fisher Thermo Scientific, Pierce) to react with the amine group of fibronectin (Sigma) to render the patterned area cell adhesive. Finally, bovine serum albumin (BSA) conjugated with Alexa Fluor 594 (Invitrogen) was doped to visualize the patterns (see Figure S11 of the Supporting Information).

**Cell Culture.** MCF-10A human epithelial cells were cultured in growth medium composed of Dulbecco's modified Eagle's medium/Ham's F-12 (DMEM/F12, Invitrogen) containing *N*-2-hydroxyethyl-piperazine-*N'*-2-ethanesulfonic acid (HEPES) and *L*-glutamine supplemented with 5% horse serum (Invitrogen), 1% penicillin/streptomycin (Invitrogen),  $10\ \mu\text{g}/\text{mL}$  insulin (Sigma),  $0.5\ \mu\text{g}/\text{mL}$  hydrocortisone (Sigma),  $20\ \text{ng}/\text{mL}$  epidermal growth factor (EGF; Peprotech) and  $0.1\ \mu\text{g}/\text{mL}$  cholera toxin (Sigma) and maintained under humidified

conditions at  $37\ ^\circ\text{C}$  and 5%  $\text{CO}_2$ . Cells were passaged regularly by dissociating confluent monolayers with 0.05% trypsin–ethylenediaminetetraacetic acid (EDTA; Invitrogen) and suspending cells in DMEM/F12 supplemented with 20% horse serum and 1% penicillin/streptomycin. Cells were passaged at 1:4 in growth medium.

**Time-Lapse Microscopy.** Cells were seeded in growth medium for 1 h on the micropatterned substrate. After several washes to remove non-adherent cells, the culture was incubated with fresh growth medium for 1 h and imaged at  $10\times$  magnification every 5 min for 12 h or at  $63\times$  magnification every 30 s for 2 h. Cells were maintained at  $37\ ^\circ\text{C}$  and 5%  $\text{CO}_2$  in a heated chamber with a temperature and  $\text{CO}_2$  controller (Pecon) during time-lapse imaging. Images and movies were acquired using an Axiovert 200 M microscope (Carl Zeiss), and Axio Vision LE Release 4.7 (Carl Zeiss) was used for image processing.

**Data Collection and Analysis.** To track cell movement on micropatterned surfaces, the position of the lamellipodial edge was tracked using Axio Vision LE Release 4.7 and ImageJ software. In the case of cells hopping at the corners of teardrop- and spear-shaped patterns, it was assumed that the cells traversed the full linear distance of the corner. Migration speed for each cell was obtained as the total distance traveled divided by the total time. The persistence length for each cell was based on the average distance traveled over multiple runs. An individual run was considered to end when the cell switched direction by  $180^\circ$  or halted to spread by extending lamella on both sides (e.g., if a cell paused to spread and then eventually proceeded in the same direction, it was counted as a separate run).

Residence times at each corner for each scenario (hop versus bounce) were tracked separately. Cells were considered as resident at a corner until their trailing edge was completely detached from that corner. Finally, directional bias was quantified as the percentage of cells that hopped in each direction, as described previously.<sup>14</sup>

**Statistical Analysis.** The unpaired, two-tailed Student's *t* test was used for statistical analysis. Differences were considered significant at *p*

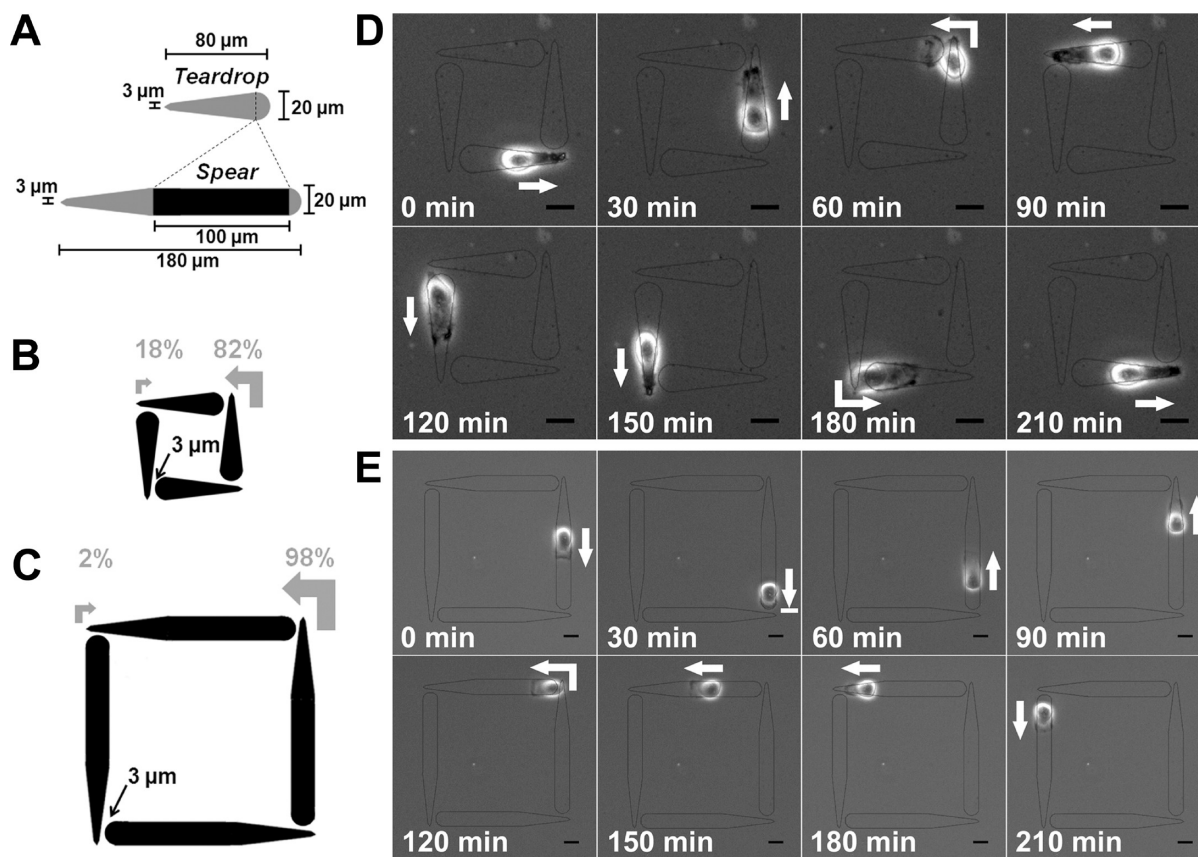


**Figure 2.** Design of a hybrid spear-shaped micropattern and its effect on the directional movement of cells. (A) Design schematic of the spear-shaped pattern. The hybrid, spear-shaped pattern is designed with an insertion of a 100  $\mu\text{m}$  long, 20  $\mu\text{m}$  wide stripe segment in the teardrop shape. The directional bias of cells moves in (B) teardrop- and (C) spear-shaped patterns. Directional bias (arrows and percentages) of spear-shaped patterns is greatly enhanced in comparison to the original teardrop patterns ( $p < 0.01$ ;  $N = 2\text{--}4$  trials with greater than 36 cells and greater than 200 jumps quantified for each pattern). Time-lapse images (extracted from Movies SI3 and SI4 of the Supporting Information) display the movement of cells on (D) teardrop- and (E) spear-shaped patterns at 30 min intervals. The white arrows indicate the direction of cell movement. Scale bar = 20  $\mu\text{m}$ .

$< 0.05$ . All of the statistical analyses were performed using corresponding functions in Microsoft Excel.

## RESULTS AND DISCUSSION

To rationally design a hybrid micropattern based on the stripe and teardrop micropatterns, we first needed to better understand the movement of cells on these building block micropatterns. We have previously quantified the movement of MCF-10A cells on teardrop-shaped micropatterns.<sup>14</sup> Thus, the initial focus of this study was to quantify the movement of MCF-10A epithelial cells on micropatterned stripes. Consistent with previous studies using NIH-3T3 fibroblasts and bovine aortic endothelial cell lines,<sup>10,11</sup> we observed that the majority of MCF-10A cells established a uniaxial migratory morphology with a single prominent lamella on one side of the cell when seeded on 10  $\mu\text{m}$  wide stripe patterns (Figure 1A). In contrast, a cell on a nonpatterned surface exhibited a broad lamella that stretched nearly across the entire width of the cell body (Figure 1B). For stripe widths ranging from 5 to 20  $\mu\text{m}$ , the cells moved  $\sim 40\text{--}50\%$  faster on micropatterned stripes (see Movie SI1 of the Supporting Information) than their counterparts on nonpatterned surfaces (see Movie SI2 of the Supporting Information) that were prepared with identical chemistry ( $p < 0.01$ ; Figure 1C). Increasing the stripe width to 30  $\mu\text{m}$  relaxed the geometric constraint such that cells no longer maintained the uniaxial morphology (Figure 1D). This loss of uniaxial

morphology coincided with a reduction in cell migration speed to a level that was statistically indistinguishable from the cell migration speed on a nonpatterned surface ( $p > 0.05$ ).

In addition to the effect of micropatterned stripes on migration speed, we observed significant enhancement in the persistence of cell migration upon confining MCF-10A cells to stripe patterns compared to cells on nonpatterned surfaces. The cells with uniaxial morphology moved approximately 250–300  $\mu\text{m}$  before flipping directions. In contrast, cells on a nonpatterned surface moved only 50  $\mu\text{m}$  on average before changing direction. As with cell speed, only stripe widths that fully confine the cell body (5–20  $\mu\text{m}$ ) resulted in this enhancement in persistence length. Taken together, our observations show that both persistence and migration speed enhancements correlate with the establishment of the uniaxial morphology and that a 20  $\mu\text{m}$  wide stripe pattern is sufficient to attain maximum improvements in speed and persistence of cell migration relative to the nonpatterned substrate.

While the 20  $\mu\text{m}$  wide stripe pattern provides significant enhancements to the speed and persistence of MCF-10A cell migration, this micropattern geometry does not control the direction in which cells travel along the stripe. That is, the physical constraint of the stripe geometry dramatically increases persistence (the tendency of cells to maintain a direction) but does not determine whether cells will move up or down the stripe pattern. In contrast, we and others have shown that

teardrop-shaped micropatterns impart a directional bias to cell movement.<sup>12,14</sup> MCF-10A cells preferentially hop from the tip end of a teardrop onto the blunt end of an adjacent island, leading cells to move in a predetermined direction.

We hypothesized that the stripe and teardrop shapes could be combined into a hybrid geometry that superimposes the enhancements in all three aspects of cell motility: speed, persistence, and directionality. To test this idea of modular engineering of micropatterns, we designed a hybrid micropattern that blended the features of the stripe and teardrop geometries and quantitatively analyzed cell migration on the hybrid micropattern. The hybrid design incorporates a 20  $\mu\text{m}$  wide stripe segment between the blunt and tip ends of the standard teardrop pattern (Figure 2A). The hybrid design yields a spear-shaped pattern that preserves the blunt and tip ends, because these features were previously shown to play a key role in determining the directional bias with which cells hop from one micropatterned island to the next. Having hopped onto an island, cells would have to traverse the middle stripe segment to reach the other end. Because cells migrate with high persistence on stripe patterns, we reasoned that cells would successfully migrate across the stripe segment without turning back, provided that the length of the segment was significantly lower than the average persistence length of cell migration on stripe patterns (300  $\mu\text{m}$ ). Thus, the length of the middle stripe segment was set to 100  $\mu\text{m}$ .

To assess the effect of the hybrid micropattern on cell motility, we analyzed and compared the migration of MCF-10A cells on teardrop-shaped (panels B and D of Figure 2 and Movie SI3 of the Supporting Information) versus spear-shaped micropatterned islands (panels C and E of Figure 2 and Movie SI4 of the Supporting Information). Both micropatterned islands were arranged to form a square-shaped “track” around which cells migrate. To ensure that any observed differences in migration could be attributed solely to the shape of each micropatterned island, the spacing and relative positioning of the islands were maintained. Time-lapse images were acquired for individual MCF-10A cells migrating on the square tracks, and the directional bias, persistence, and speed of MCF-10A cell movement were quantified.

We first sought to confirm that the directional bias of cell migration exhibited on the original teardrop micropattern was not compromised by the addition of the middle stripe segment. Unexpectedly, cell migration on the hybrid spear-shaped micropattern exhibited even greater directional bias than on the original teardrop design. On the hybrid spear micropattern, cells moved from island to island, with 98% of the hops favoring the tip-to-blunt direction, while only 2% of the successful hops occurred in the blunt-to-tip direction (Figure 2C). Meanwhile, on the standard teardrop-shaped micropattern, the bias for the tip-to-blunt hops was only 82% (Figure 2B).

This enhancement in the directional bias was unexpected because the local topography where the hopping takes place (blunt and tip ends) was unaltered between the two patterns and the inserted stripe pattern is directionally unbiased. To better understand this synergistic improvement, we quantified the “decision” that cells make at each end of the spear- and teardrop-shaped micropatterns. On each end (tip or blunt), we quantified the likelihood that a cell hops to the adjacent island (successful hop) as opposed to “bouncing” by turning back to migrate down the island (Table 1). On the tip end of teardrop micropatterns, the hop probability was 73%. In contrast, the

**Table 1. Detailed Analysis of Hop Decisions at Corners**

tip end	teardrop-shaped pattern		spear-shaped pattern	
	occurrences	probability (%)	occurrences	probability (%)
successful hop	208	73	166	97
bounce	78	27	6	3
blunt end	teardrop-shaped pattern		spear-shaped pattern	
	occurrences	probability (%)	occurrences	probability (%)
successful hop	45	38	4	15
bounce	73	62	23	85

hop probability improved to 97% on the tip end of spear-shaped micropatterns. Furthermore, the likelihood that a cell hopped on the blunt end decreased from 38% on teardrop patterns to 15% on the hybrid spear patterns. Thus, the inclusion of a middle stripe segment in the teardrop pattern not only improved the likelihood of a hop at the tip end but also reduced the probability that a cell would hop at the blunt end. Therefore, improvements in cell fate choices at both ends of the spear pattern together contribute to the marked enhancement in the directional bias of cell movement.

In addition to directional bias, our quantitative analysis showed that the tendency of cells to maintain the direction of movement increased on the hybrid spear micropattern compared to the original teardrop pattern. The average distance cells moved before changing direction on the original teardrop patterns was 383  $\mu\text{m}$ . On the spear-shaped micropattern, the persistence length increased by 141% to 925  $\mu\text{m}$  (see Table SI1 of the Supporting Information).

To understand better the observed increase in persistence on hybrid micropatterns, we examined the persistence of cell movement on stripes and teardrops. On the standard 80  $\mu\text{m}$  long teardrop shapes, the persistence of cell movement was approximately 383  $\mu\text{m}$  or 4.79 teardrops. Because the hybrid design incorporated a stripe segment with a length (100  $\mu\text{m}$ ) significantly below the migration persistence on a stripe pattern, we reasoned that cells would maintain their direction of movement along this 100  $\mu\text{m}$  segment in the middle of the spear-shaped pattern. Hence, under a purely modular view, the persistence on the hybrid pattern would be predicted to be  $(80 + 100) \mu\text{m}/\text{teardrop} \times 4.79 \text{ teardrops} = 862 \mu\text{m}$  (Figure 3A). This predicted persistence differs from the measured persistence (925  $\mu\text{m}$ ) only by  $\sim 7\%$ . This analysis reveals that the stripe and teardrop shapes provide quantitatively modular contributions to the persistence of cell migration, such that a hybrid pattern yields an approximately additive and predictable improvement in this aspect of cell migration.

Finally, we assessed the effect of the hybrid micropattern design on the cell migration speed. Because cell speed on stripe patterns is similar to that on teardrop patterns (98.8  $\mu\text{m}/\text{h}$  on stripe and 91.0  $\mu\text{m}/\text{h}$  on teardrop), inserting a stripe segment into the teardrop pattern was not expected to affect the cell migration speed. Quantitative analysis of time-lapse movies, however, revealed that the average cell speed on spear-shaped micropatterns was 121  $\mu\text{m}/\text{h}$ , a 33% improvement compared to teardrop micropatterns (see Table SI1 of the Supporting Information).

To understand better this unexpected improvement in cell speed, we examined more closely the events at the corners of the square track where cells hop from one island to the next. We reasoned that the spear-shaped pattern might improve the

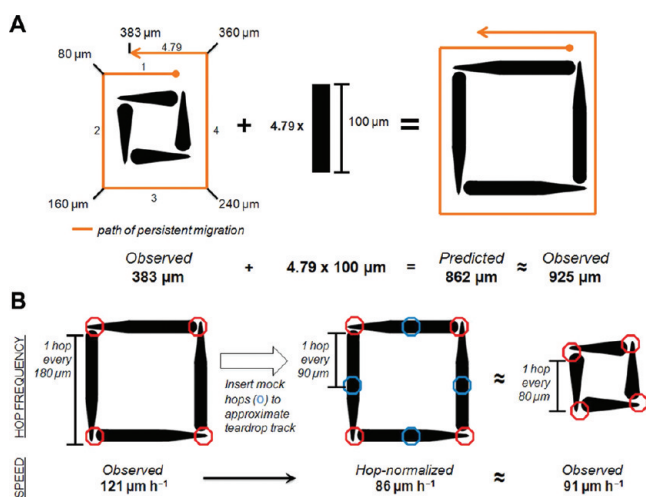


**Figure 3.** Modular enhancement of the persistence length and migration speed on the hybrid spear-shaped micropattern. (A) Prediction of the persistence length on the spear-shaped pattern based on the measured persistence on teardrop and stripe patterns. (B) Calculations to normalize the observed cell speed on spear-shaped micropatterns for the frequency of hops (red circles). Mock hops (blue circles) were inserted into the spear-shaped pattern to render the hop frequency equivalent to that of teardrop patterns.

average migration speed by reducing the amount of time for cells to hop at each corner. To test this possibility, we quantified the residence time of cells at the corners of the square track during tip-to-blunt and blunt-to-tip hops (see Figure SI2 of the Supporting Information). Residence times on spear-shaped patterns seemed on average shorter than those on teardrop patterns. The average residence times spent at the tip end were 29 and 40 min on spear and teardrop patterns, respectively, while the times spent at the blunt end were 34 and 46 min on spear and teardrop patterns, respectively. However, these differences in hop duration were not statistically significant ( $p > 0.05$ ), and thus, the residence times at the corners of the square track were not sufficient to explain the differences in migration speeds between spear and teardrop patterns.

While the residence times at corners are not statistically different between teardrop and spear micropatterns, our measurements raised an alternate hypothesis (Figure 3B). Because hops take on average 37 min on spear and teardrop patterns, they represent a significant fraction of the time that a cell spends in traversing around the square track. For example, cells take 3.5 h to traverse a four teardrop track ( $4 \times 80 \mu\text{m} \div 91 \mu\text{m/h}$ ), of which approximately  $37 \text{ min} \times 4 \approx 2.5 \text{ h}$  is spent hopping at the corners. Thus, the number of hops that a cell has to execute to traverse the track contributes significantly to the average migration speed. It is evident that, on the teardrop pattern, a hop must be executed every  $80 \mu\text{m}$ ; in contrast, on the spear-shaped pattern, hop events are spaced further apart ( $180 \mu\text{m}$ ). Thus, the frequency of hops is approximately 2-fold greater on teardrop patterns and could account for the apparent lower migration speed on teardrop-based tracks than on the spear-based counterparts.

To analyze this idea more quantitatively, we estimated the average migration speed of a cell traversing a theoretical spear-based track in which the frequency of hops were doubled. The time that a cell would take to transit this theoretical spear-shaped pattern is the time to transit the actual spear-shaped

micropattern ( $180 \mu\text{m} \div 121 \mu\text{m/h} = 1.5 \text{ h}$ ) plus the time needed to execute a mock hop (37 min). The predicted traversal time of 2.1 h translates to an estimated migration speed of  $180 \mu\text{m} \div 2.1 \text{ h} = 86 \mu\text{m/h}$ . This hop-normalized migration speed deviates only 5% from the speed observed on the teardrop-shaped pattern ( $91 \mu\text{m/h}$ ).

Therefore, we conclude that the hybrid spear-shaped micropattern improves cell migration speed not by enhancing cell migration or reducing the time that it takes for cells to hop but by requiring fewer hops per unit length, owing to the insertion of a stripe segment in the base teardrop pattern. Furthermore, our analysis shows that the effect of the hybrid design on the cell migration speed is modular and can be understood quantitatively as the sum of contributions from the stripe and teardrop micropatterns.

## CONCLUSION

The findings in this study show that two “building block” micropattern motifs, teardrops and stripes, can be combined to design a hybrid micropattern that achieves combinatorial, multifaceted enhancements in cell motility. The hybrid spear-shaped micropattern design combines the enhanced cell migration speed and persistence provided by stripe patterns and the directional bias provided by teardrop patterns. By inserting a stripe segment into the original teardrop pattern, we exploit the remarkably high persistence of cell migration on stripe patterns. Thus, the directional bias conferred by each hop is capitalized over longer linear runs before the next junction is required to re-establish and maintain the bias in movement.

In addition to achieving multifaceted improvements in motility, the hybrid design exhibits modular behavior. The speed and persistence of cell migration on spear-shaped patterns are related directly and quantitatively to the migratory behavior on stripe and teardrop micropatterns. However, this modular predictability does not extend to all facets of motility. Directional bias on spear-shaped micropatterns exhibits an unexpected improvement relative to the teardrop design. Thus, there are clearly synergistic interactions when stripe and teardrop motifs are combined into a hybrid design. Future work will test the extensibility of this modular approach to additional building-block micropatterns. Elucidating how foundational micropattern geometries can be mixed and matched to engineer multifunctional hybrid patterns will offer principles for the design of higher order geometric cues to control cell behavior on “smart” biomaterials.

## ASSOCIATED CONTENT

### Supporting Information

Figures showing the residence times at the tip end and blunt end of teardrop- and spear-shaped patterns, visualization of the underlying pattern through BSA-Cy3, table of speed and persistence of cell migration on teardrop- and spear-shaped patterns, and AVI movies of cells migrating on nonpattern,  $10 \mu\text{m}$  wide stripe pattern, teardrop-shaped pattern, and spear-shaped pattern. This material is available free of charge via the Internet at <http://pubs.acs.org>.

## AUTHOR INFORMATION

### Corresponding Author

\*Telephone: (617) 373-2996. E-mail: [anand@cell-engineering.org](mailto:anand@cell-engineering.org).

## Notes

The authors declare no competing financial interest.

## ■ ACKNOWLEDGMENTS

This research was funded by National Institutes of Health (NIH) R01-CA138899, the National Cancer Institute (NCI)–University of Southern California (USC) Physical Sciences of Oncology Center (U54CA143907), and the National Science Foundation (NSF) Center for Science and Engineering of Materials at the California Institute of Technology. We also gratefully acknowledge the technical support and infrastructure provided by the Kostas Facility for Micro and Nanofabrication at Northeastern University and the Kavli Nanoscience Institute at the California Institute of Technology.

## ■ REFERENCES

- (1) Lee, S. H.; Moon, J. J.; West, J. L. *Biomaterials* **2008**, *29*, 2962–2968.
- (2) Raghavan, S.; Nelson, C. M.; Baranski, J. D.; Lim, E.; Chen, C. S. *Tissue Eng., Part A* **2010**, *16*, 2255–2263.
- (3) Thery, M. J. *Cell Sci.* **2010**, *123*, 4201–4213.
- (4) Brunette, D. M. *Exp. Cell Res.* **1986**, *167*, 203–217.
- (5) Clark, P.; Connolly, P.; Curtis, A. S.; Dow, J. A.; Wilkinson, C. D. *J. Cell Sci.* **1991**, *99*, 73–77.
- (6) Tan, J.; Saltzman, W. M. *Biomaterials* **2002**, *23*, 3215–3225.
- (7) Gao, D.; Kumar, G.; Co, C.; Ho, C. C. *Adv. Exp. Med. Biol.* **2008**, *614*, 199–205.
- (8) Clark, P.; Britland, S.; Connolly, P. *J. Cell Sci.* **1993**, *105*, 203–212.
- (9) Szabo, B.; Kornyei, Z.; Zach, J.; Selmeczi, D.; Csucs, G.; Czirok, A.; Vicsek, T. *Cell Motil. Cytoskeleton* **2004**, *59*, 38–49.
- (10) Li, S.; Bhatia, S.; Hu, Y. L.; Shin, Y. T.; Li, Y. S.; Usami, S.; Chien, S. *Biorheology* **2001**, *38*, 101–108.
- (11) Doyle, A. D.; Wang, F. W.; Matsumoto, K.; Yamada, K. M. *J. Cell Biol.* **2009**, *184*, 481–490.
- (12) Kumar, G.; Ho, C. C.; Co, C. C. *Adv. Mater.* **2007**, *19*, 1084–1090.
- (13) Mahmud, G.; Campbell, C. J.; Bishop, K. J. M.; Komarova, Y. A.; Chaga, O.; Soh, S.; Huda, S.; Kandere-Grzybowska, K.; Grzybowski, B. A. *Nat. Phys.* **2009**, *5*, 606–612.
- (14) Kushiro, K.; Chang, S.; Asthagiri, A. R. *Adv. Mater.* **2010**, *22*, 4516–4519.
- (15) Kumar, G.; Co, C. C.; Ho, C. C. *Langmuir* **2011**, *27*, 3803–3807.
- (16) Jiang, X.; Bruzewicz, D. A.; Wong, A. P.; Piel, M.; Whitesides, G. M. *Proc. Natl. Acad. Sci. U.S.A.* **2005**, *102*, 975–978.
- (17) Woodard, A. S.; Garcia-Cardena, G.; Leong, M.; Madri, J. A.; Sessa, W. C.; Languino, L. R. *J. Cell Sci.* **1998**, *111*, 469–478.
- (18) Maheshwari, G.; Wells, A.; Griffith, L. G.; Lauffenburger, D. A. *Biophys. J.* **1999**, *76*, 2814–2823.